ChemComm

COMMUNICATION

View Article Online
View Journal | View Issue

Cite this: *Chem. Commun.*, 2018, **54**, 13678

Received 25th October 2018,
Accepted 6th November 2018

DOI: 10.1039/c8cc08553f

rsc.li/chemcomm

A dual signal amplification-assisted DNAzyme biosensor for ultrasensitive detection of Argonaute 2 activity†

Dandan Zhang,‡[a] Fei Ma,‡[a] Junhong Leng‡[b] and Chun-yang Zhang *[a]

We develop a new DNAzyme biosensor for Argonaute 2 (Ago2) assay based on target-initiated rolling circle amplification in combination with an 8-17 DNAzyme-mediated dual signal amplification strategy. This biosensor can achieve ultrahigh sensitivity with a detection limit of 0.35 pM, and it can be further used for the screening of Ago2 inhibitors and the accurate measurement of endogenous Ago2 from HeLa cell extracts.

Argonaute proteins are essential elements of RNA-induced silencing complexes (RISC) in eukaryotic cells, participating in RNA-mediated gene silencing processes.[1] The Ago proteins can firstly bind with small non-coding RNAs (*e.g.* microRNAs and small interfering RNAs) to form an active RISC structure which is able to cleave the target messenger RNA (mRNA) to cause gene silencing.[2] Ago protein-mediated transcriptional regulations play critical roles in many biological processes, including cell development, proliferation, differentiation, and hematopoiesis.[3] Moreover, the dysregulation of cellular Argonaute levels has been closely associated with various human diseases including cancers,[4] and human Argonaute 2 (Ago2) is over-expressed in colon cancer,[5] cervical cancer,[6] ovarian carcinoma,[7] and gastric carcinoma.[8] Therefore, the accurate detection of Argonaute proteins is crucial for both Argonaute- and gene silencing-associated biological studies and disease diagnosis.

The antibody-based Western blotting (WB)[9] and enzyme-linked immunosorbent assay (ELISA)[10] are most widely used for Argonaute assay; however, they usually suffer from laborious and time-consuming procedures. In addition, these methods are only suitable for detecting the protein contents of Argonaute instead of its cleavage activity towards the target RNA. To solve these issues, some alternative methods have been established, such as G-quadruplex-based electrochemical assay[11] and molecular beacon-based fluorescence assay.[12] Despite their good performance in selectivity, reproducibility and simplicity, the sensitivities of these methods are quite limited due to the lack of an efficient signal amplification strategy. Therefore, there is an urgent need for the development of new methods for Argonaute activity assay with improved sensitivity.

Deoxyribozymes (DNAzymes) are a type of functional nucleic acid that catalyzes many biological reactions including RNA cleavage,[13] RNA ligation,[14] and oxidation–reduction reactions.[15] Superior to the conventional protein-based enzymes, DNAzymes are highly stable, highly active, and cost effective,[16] making them attractive elements for the construction of efficient biosensors for the detection of DNAs,[17] microRNAs,[18] proteins,[19] enzymes,[20] and metal ions.[21] To the best of our knowledge, the development of a DNAzyme biosensor for Argonaute assay has not yet been reported so far, probably due to the inability of Argonaute to induce the generation of DNAzyme directly. Rolling circle amplification (RCA) is a highly efficient nucleic acid amplification approach that can produce long single-stranded DNAs by using a suitable DNA polymerase with strand displacement activity,[22] and it has been widely used for the detection of various biomolecules including DNAs,[23] microRNAs,[24] proteins,[25] and enzymes.[26] Especially, RCA can efficiently synthesize the repetitive sequences of functional nucleic acids including DNAzymes,[27] greatly extending RCA-based biosensing applications and improving the assay sensitivity.[28]

In this research, we develop a new DNAzyme biosensor for Argonaute 2 (Ago2) activity assay by the combination of a target-initiated RCA reaction with 8-17 DNAzyme-mediated dual signal amplification. Among various DNAzymes, 8-17 DNAzyme is the most extensively used metalloenzyme, and it can catalyze the cleavage of RNA strands with divalent metal ions (*e.g.*, Zn^{2+}, Mg^{2+}, and Pb^{2+}) as the cofactors.[29] As shown in Scheme 1, a single-stranded substrate RNA (sRNA) is employed to sense the

[a] *College of Chemistry, Chemical Engineering and Materials Science, Collaborative Innovation Center of Functionalized Probes for Chemical Imaging in Universities of Shandong, Key Laboratory of Molecular and Nano Probes, Ministry of Education, Shandong Provincial Key Laboratory of Clean Production of Fine Chemicals, Shandong Normal University, Jinan 250014, China. E-mail: cyzhang@sdnu.edu.cn; Fax: +86 0531-82615258; Tel: +86 0531-86186033*

[b] *Jinan Maternity and Child Care Hospital, Jinan 250000, China*

† Electronic supplementary information (ESI) available. See DOI: 10.1039/c8cc08553f

‡ These authors contributed equally.

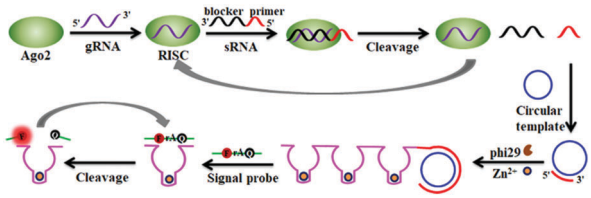

Scheme 1 Schematic illustration of the DNAzyme biosensor for Ago2 assay based on target-initiated rolling circle amplification in combination with an 8-17 DNAzyme-mediated dual signal amplification strategy.

target Ago2. This sRNA contains a primer sequence (Scheme 1, red color) at its 5′ region and a blocker sequence at its 3′ region (Scheme 1, black color). The primer is fully complementary to the circular template (Scheme 1, blue) and it may function as a trigger to initiate the RCA reaction, while the blocker is non-complementary to the circular template and it can prohibit the nonspecific RCA reaction when the target is absent. In the presence of target Ago2, Ago2 will bind with the guide RNA (gRNA, Scheme 1, purple color) to form an active RNA-induced silencing complex (RISC) which subsequently cleaves the sRNA to release the free primer sequence from the intact sRNA. Notably, the RISC can be recycled to initiate the next cycle of sRNA cleavage, producing abundant free primers. The free primer can bind with the circular template to initiate the RCA reaction with the assistance of phi29 DNA polymerase. As a result, a long repetitive single-stranded DNA containing 18-7 DNAzymes (Scheme 1, pink color) is synthesized. A FAM (F) and BHQ1 (Q) dual-labeled signal probe (Scheme 1, blue color) containing a single ribonucleotide (rA) is employed to sense the 8-17 DNAzyme. In the absence of 8-17 DNAzyme, the signal probe remains intact with the fluorescence of FAM being efficiently quenched by BHQ1 as a result of the fluorescence resonance energy transfer (FRET) effect,[30] leading to a low background signal. In the presence of target Ago2, the RCA-generated 8-17 DNAzyme possesses the ribonuclease activity with Zn^{2+} as the cofactor, and it can catalyze the cleavage of the signal probe into two pieces at the rA position, resulting in the spatial separation of FAM from BHQ1 and consequently the recovery of the FAM fluorescence signal. Notably, the released 8-17 DNAzyme can bind with another signal probe to initiate a new round of cleavage reaction, leading to an enhanced FAM fluorescence signal. In contrast, in the absence of target Ago2, the sRNA cannot be cleaved for the initiation of the RCA reaction, and consequently no DNAzyme is produced for the cleavage of signal probes and no enhanced FAM fluorescence signal is observed. Due to the highly efficient target-triggered RCA and the 8-17 DNAzyme-mediated dual signal amplification, this biosensor enables selective detection of Ago2 activity with ultrahigh sensitivity.

We performed fluorescence measurements to verify the feasibility of the proposed strategy for Ago2 assay. As shown in Fig. 1, in the presence of Ago2, gRNA, and sRNA (Fig. 1, red line), a high fluorescence signal with the characteristic emission peak at 512 nm is observed, indicating the target-triggered dual signal amplification-induced cleavage of signal probes and the

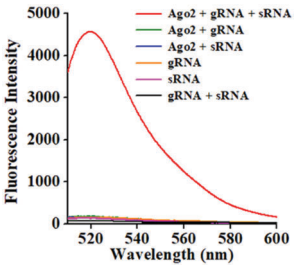

Fig. 1 Fluorescence emission spectra of FAM in response to Ago2 + gRNA + sRNA (red line), Ago2 + gRNA (green line), Ago2 + sRNA (blue line), gRNA (yellow line), sRNA (pink line), and gRNA + sRNA (black line). 1 μM Ago2, 200 nM gRNA and 600 nM sRNA were used in this experiment.

recovery of the FAM signal. In contrast, when Ago2 is absent, no distinct fluorescence signal is observed in the presence of gRNA (Fig. 1, yellow line), sRNA (Fig. 1, pink line), and gRNA + sRNA (Fig. 1, black line), suggesting no occurrence of signal amplification without Ago2. In addition, no distinct fluorescence signal is produced in response to only Ago2 + gRNA (Fig. 1, green line) because no available sRNA can be cleaved for the production of a free RCA primer. Notably, the presence of Ago2 and sRNA without gRNA (Fig. 1, blue line) cannot generate a distinct fluorescence signal either, suggesting that gRNA is a necessary component for the formation of an active RISC which can cleave sRNA to trigger the subsequent dual signal amplification reactions.

To evaluate the sensitivity of the proposed biosensor, we measured the FAM fluorescence emission spectra in response to different concentrations of Ago2 from 0 to 1 μM (Fig. 2A) under optimal experimental conditions including the Ago2 incubation time of 30 min, 90 nM circular template, 1.2 U of phi29 DNA polymerase, 1.2 μM signal probe, a RCA reaction time of 120 min, and 20 μM Zn^{2+} (see Fig. S1, ESI†). In the logarithmic scale, the fluorescence intensity exhibits a linear correlation with the concentration of Ago2 over a range of 6 orders of magnitude from 1 pM to 1 μM (Fig. 2B). The regression equation is $F = 8307.82 + 682.99 \log_{10} C$ with a correlation coefficient (R^2) of 0.9954, where F and C represent the fluorescence intensity and the concentration of Ago2 (M), respectively. The limit of detection is calculated to be 0.35 pM by evaluating the average signal of the blank plus three times the standard deviation.

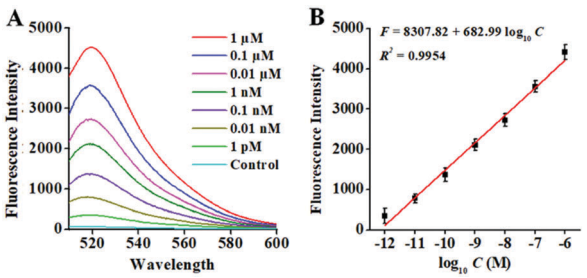

Fig. 2 (A) Measurement of FAM fluorescence emission spectra in response to different concentrations of Ago2 from 0 (control) to 1 μM. (B) Linear relationships between the fluorescence intensity and the logarithm of Ago2 concentration from 1 pM to 1 μM. Error bars show the standard deviation of three experiments.

Notably, the sensitivity of the proposed biosensor has improved by as much as 3 orders of magnitude compared with that of RNA molecular beacon-based fluorescent assay (0.6 nM)[12a] and 4 orders of magnitude compared with that of graphene oxide-based fluorescent assay (1.7 nM),[12b] and the electrochemical assay (5.02 nM).[11] The extremely high sensitivity of this biosensor may be ascribed to the efficient dual signal amplification strategy including the target-induced RCA amplification and the 8-17 DNAzyme-assisted cyclical signal amplification (Scheme 1).

To investigate the specificity of the proposed biosensor, we used thrombin, bovine serum albumin (BSA), and hemoglobin as the nonspecific proteins. In theory, none of the above proteins can interact with gRNA to form an active RISC, and thus no 8-17 DNAzyme can be synthesized by RCA and no distinct fluorescence signal can be detected. As expected, no distinct fluorescence signal is produced in response to thrombin (Fig. 3, green column), BSA (Fig. 3, blue column), hemoglobin (Fig. 3, pink column), and the control without any proteins (Fig. 3, black column). In contrast, a significantly enhanced fluorescence signal is detected in response to target Ago2 (Fig. 3, red column), and its fluorescence intensity is 59.1-, 31.5-, and 28-fold higher than those produced by thrombin, BSA and hemoglobin, respectively. These results clearly demonstrated the high selectivity of the proposed biosensor towards Ago2.

To investigate the capability of the proposed biosensor for Ago2 inhibition assay, we used aurintricarboxylic acid (ATA) as the potential Ago2 inhibitor. The ATA can efficiently inhibit Ago2 activity by preventing the binding of gRNA with the Ago2 protein to disturb the formation of an RISC.[31] The relative activity of Ago2 (RA) was measured according to eqn (1):

$$\mathrm{RA}\ (\%) = \frac{F_i - F_0}{F_t - F_0} \times 100\% \qquad (1)$$

where F_0 is the fluorescence intensity in the absence of Ago2, F_t is the fluorescence intensity in the presence of 1 μM Ago2, and F_i is the fluorescence intensity in the presence of both Ago2 and ATA. As shown in Fig. 4, the relative activity of Ago2 decreases with the increase of ATA concentration from 0 to 10 μM. The IC_{50} value (defined as the inhibitor concentration required to reduce the enzyme activity by 50%) is estimated to be 0.45 μM, consistent with that obtained by the fluorescence polarization assay (0.47 μM).[31] This result indicates that the proposed biosensor can be applied for the screening of Ago2 inhibitors.

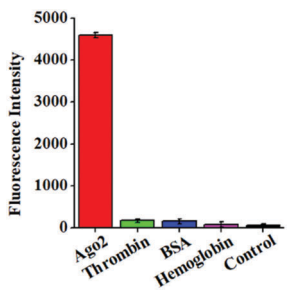

Fig. 3 Measurement of FAM fluorescence signal in response to 1 μM Ago2 (red column), 1 μM thrombin (green column), 1 μM BSA (blue column), 1 μM hemoglobin (pink column), and the control without any proteins (black column). Error bars show the standard deviation of three experiments.

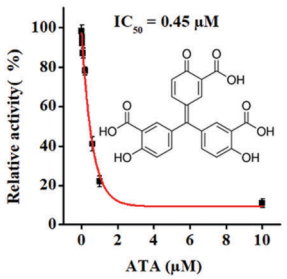

Fig. 4 Variance of the relative activity of Ago2 in response to different concentrations of ATA from 0 to 10 μM. The Ago2 concentration is 1 μM. Error bars show the standard deviations of three experiments. The inset shows the chemical structure of ATA.

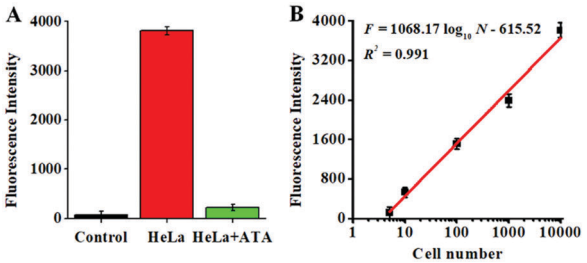

Fig. 5 (A) Measurement of FAM fluorescence intensity in response to the control without any cell extracts (black column), HeLa cells (red column), and HeLa cells + ATA (green column). Cell extracts equivalent to 10 000 HeLa cells and 20 μM ATA were used in this experiment. (B) Linear relationship between the FAM fluorescence intensity and the logarithm of the number of HeLa cells from 5 to 10 000 cells. Error bars show the standard deviations of three independent experiments.

Ago2 is widely expressed in eukaryotic cells.[32] To investigate the feasibility of the proposed biosensor for real sample analysis, we measured the Ago2 activity in human cervical cancer cells (HeLa cells) which were obtained from the Cell Bank, Shanghai Institutes for Biological Sciences, Chinese Academy of Sciences (Shanghai, China) (Fig. 5A). In contrast to the low background signal from the control without any cell extracts (Fig. 5A, black column), an obviously enhanced fluorescence signal is generated in the presence of HeLa cell extracts (Fig. 5A, red column). Notably, the addition of the Ago2 inhibitor ATA to the HeLa cells induces a significant decrease in the fluorescence signal (Fig. 5A, green column) due to the inhibition of the Ago2 activity by ATA (Fig. 4). Moreover, in the logarithmic scale, the fluorescence intensity exhibits a linear correlation with the HeLa cell number from 5 to 10 000 cells (Fig. 5B). The equation is $F = 1068.17 \log_{10} N - 615.52$ with a correlation coefficient (R^2) of 0.991, where F is the fluorescence intensity and N is the number of HeLa cells, respectively. The limit of detection is calculated to be 3 cells by evaluating the average response of the control group plus 3 times the standard deviation. These results clearly demonstrated that the proposed biosensor can be used to monitor the endogenous Ago2 activity in complex biological samples.

In conclusion, we have developed a new dual-signal amplification-assisted DNAzyme biosensor for Ago2 activity assay.

The presence of the target Ago2 can induce the cleavage of the substrate RNA to generate a free RCA primer which can initiate the RCA reaction to synthesise large amounts of 8-17 DNAzymes, and the resultant 8-17 DNAzymes can cyclically digest abundant signal probes to produce an amplified fluorescence signal. Due to the introduction of the dual signal amplification strategy, the proposed DNAzyme biosensor can sensitively detect Ago2 activity with a detection limit as low as 0.35 pM, and it can even accurately measure the endogenous Ago2 activity from HeLa cell extracts with a detection limit of 3 cells. This biosensor can be further applied for the screening of Ago2 inhibitors, holding great potential in Ago2-related fundamental research and clinical applications.

This work was supported by the National Natural Science Foundation of China (Grant No. 21325523, 21527811, 21735003 and 21705096) and the Award for Team Leader Program of Taishan Scholars of Shandong Province, China.

Conflicts of interest

There are no conflicts to declare.

Notes and references

1 (*a*) A. Boland, F. Tritschler, S. Heimstädt, E. Izaurralde and O. Weichenrieder, *EMBO Rep.*, 2010, **11**, 522–527; (*b*) D. H. Kim, L. M. Villeneuve, K. V. Morris and J. J. Rossi, *Nat. Struct. Mol. Biol.*, 2006, **13**, 793; (*c*) G. Meister and T. Tuschl, *Nature*, 2004, **431**, 343.
2 (*a*) G. Meister, *Nat. Rev. Genet.*, 2013, **14**, 447; (*b*) H.-o. Iwakawa and Y. Tomari, *Trends Cell Biol.*, 2015, **25**, 651–665; (*c*) E. J. Sontheimer and R. W. Carthew, *Science*, 2004, **305**, 1409–1410.
3 (*a*) G. Stefani and F. J. Slack, *Nat. Rev. Mol. Cell Biol.*, 2008, **9**, 219; (*b*) A. Mallory and H. Vaucheret, *Plant Cell*, 2010, **22**, 3879–3889; (*c*) T. M. T. Hall, *Structure*, 2005, **13**, 1403–1408; (*d*) D. O'Carroll, I. Mecklenbrauker, P. P. Das, A. Santana, U. Koenig, A. J. Enright, E. A. Miska and A. Tarakhovsky, *Genes Dev.*, 2007, **21**, 1999–2004.
4 Z. Ye, H. Jin and Q. Qian, *J. Cancer*, 2015, **6**, 877–882.
5 L. Li, C. Yu, H. Gao and Y. Li, *BMC Cancer*, 2010, **10**, 38.
6 J. Guo, J. Lv, M. Liu and H. Tang, *J. Biol. Chem.*, 2015, **290**, 30342–30350.
7 O. Vaksman, T. E. Hetland, C. G. Trope, R. Reich and B. Davidson, *Hum. Pathol.*, 2012, **43**, 2062–2069.
8 J. Zhang, X.-s. Fan, C.-x. Wang, B. Liu, Q. Li and X.-j. Zhou, *Med. Oncol.*, 2013, **30**, 628.
9 K. Okamura, A. Ishizuka, H. Siomi and M. C. Siomi, *Genes Dev.*, 2004, **18**, 1655–1666.
10 K. Ikeda, M. Satoh, K. M. Pauley, M. J. Fritzler, W. H. Reeves and E. K. L. Chan, *J. Immunol. Methods*, 2006, **317**, 38–44.
11 N. Yang, Y. Cao, P. Han, X. Zhu, L. Sun and G. Li, *Anal. Chem.*, 2012, **84**, 2492–2497.
12 (*a*) F. Li, P. Li, L. Yang and B. Tang, *Chem. Commun.*, 2012, **48**, 12192–12194; (*b*) F. Li, M. Chen, X. Sun, X. Wang and P. Li, *Sens. Actuators, B*, 2013, **182**, 156–160.
13 S. W. Santoro, G. F. Joyce, K. Sakthivel, S. Gramatikova and C. F. Barbas, *J. Am. Chem. Soc.*, 2000, **122**, 2433–2439.
14 A. Flynn-Charlebois, Y. Wang, T. K. Prior, I. Rashid, K. A. Hoadley, R. L. Coppins, A. C. Wolf and S. K. Silverman, *J. Am. Chem. Soc.*, 2003, **125**, 2444–2454.
15 Y. Yuan, Y. Chai, R. Yuan, Y. Zhuo and X. Gan, *Chem. Commun.*, 2013, **49**, 7328–7330.
16 (*a*) Y. Tian, Y. He, Y. Chen, P. Yin and C. Mao, *Angew. Chem.*, 2005, **117**, 4429–4432; (*b*) S. K. Silverman, *Acc. Chem. Res.*, 2009, **42**, 1521–1531.
17 M. Luo, X. Chen, G. Zhou, X. Xiang, L. Chen, X. Ji and Z. He, *Chem. Commun.*, 2012, **48**, 1126–1128.
18 P. Zhang, X. Wu, R. Yuan and Y. Chai, *Anal. Chem.*, 2015, **87**, 3202–3207.
19 Y. Huang, J. Chen, S. Zhao, M. Shi, Z.-F. Chen and H. Liang, *Anal. Chem.*, 2013, **85**, 4423–4430.
20 (*a*) X.-H. Zhao, L. Gong, X.-B. Zhang, B. Yang, T. Fu, R. Hu, W. Tan and R. Yu, *Anal. Chem.*, 2013, **85**, 3614–3620; (*b*) F. Ma, Y. Yang and C.-y. Zhang, *Anal. Chem.*, 2014, **86**, 6006–6011.
21 B.-C. Yin, B.-C. Ye, W. Tan, H. Wang and C.-C. Xie, *J. Am. Chem. Soc.*, 2009, **131**, 14624–14625.
22 (*a*) W. Zhao, M. M. Ali, M. A. Brook and Y. Li, *Angew. Chem., Int. Ed.*, 2008, **47**, 6330–6337; (*b*) M. Liu, J. Song, S. Shuang, C. Dong, J. D. Brennan and Y. Li, *ACS Nano*, 2014, **8**, 5564–5573.
23 P. M. Lizardi, X. Huang, Z. Zhu, P. Bray-Ward, D. C. Thomas and D. C. Ward, *Nat. Genet.*, 1998, **19**, 225.
24 Y. Cheng, X. Zhang, Z. Li, X. Jiao, Y. Wang and Y. Zhang, *Angew. Chem., Int. Ed.*, 2009, **48**, 3268–3272.
25 B. Schweitzer, S. Roberts, B. Grimwade, W. Shao, M. Wang, Q. Fu, Q. Shu, I. Laroche, Z. Zhou, V. T. Tchernev, J. Christiansen, M. Velleca and S. F. Kingsmore, *Nat. Biotechnol.*, 2002, **20**, 359.
26 F. Ma, S.-h. Wei, J. Leng, B. Tang and C.-y. Zhang, *Chem. Commun.*, 2018, **54**, 2483–2486.
27 (*a*) M. M. Ali and Y. Li, *Angew. Chem.*, 2009, **121**, 3564–3567; (*b*) F. Wang, C.-H. Lu, X. Liu, L. Freage and I. Willner, *Anal. Chem.*, 2014, **86**, 1614–1621.
28 (*a*) Y. Wen, Y. Xu, X. Mao, Y. Wei, H. Song, N. Chen, Q. Huang, C. Fan and D. Li, *Anal. Chem.*, 2012, **84**, 7664–7669; (*b*) S. Bi, L. Li and S. Zhang, *Anal. Chem.*, 2010, **82**, 9447–9454; (*c*) J. Zhuang, W. Lai, G. Chen and D. Tang, *Chem. Commun.*, 2014, **50**, 2935–2938.
29 H.-K. Kim, J. Liu, J. Li, N. Nagraj, M. Li, C. M. B. Pavot and Y. Lu, *J. Am. Chem. Soc.*, 2007, **129**, 6896–6902.
30 F. Ma, W.-j. Liu, L. Liang, B. Tang and C.-Y. Zhang, *Chem. Commun.*, 2018, **54**, 2413–2416.
31 G. S. Tan, C.-H. Chiu, B. G. Garchow, D. Metzler, S. L. Diamond and M. Kiriakidou, *ACS Chem. Biol.*, 2012, **7**, 403–410.
32 C.-D. Kuhn and L. Joshua-Tor, *Trends Biochem. Sci.*, 2013, **38**, 263–271.